



Flexible modified plastic strips coated polyaniline/graphene composite for electrochemical biosensors

Sangeetha D. N.^a, Pooja H^a, Savisha Bhandary^a, Yashaswini Shetty^a, Raghu Subashchandrabose^b & M. Selvakumar^{a,*}

^aDepartment of chemistry, Manipal Institute of Technology, Manipal Academy of Higher Education, Manipal 576104, India

^bCARD/Chemistry, Vistas-Vels University, Pallavaram, Chennai 600 117, India

E-mail: chemselva78@gmail.com

Received 14 August 2019; revised and accepted 20 April 2020

Polyaniline(PANI)/graphene modified flexible, disposable polyester overhead projector (OHP) strips for non-enzymatic detection of ascorbic acid (AA) and uric acid (UA) is demonstrated in the current work. The deposition of PANI on the 3-aminopropyltrimethoxy silane (APTMS) modified OHP have been optimized through electrochemical impedance spectroscopy. Graphene is coated on another end. The PANI/graphene coating is confirmed through scanning electron microscopy. UA and AA detection have been carried out using the standard electrochemical techniques like cyclic voltammetry and chronoamperometry. The study reveals that the composite of PANI/graphene exhibits good sensing towards the detection of UA and AA. During the detection of UA and AA, PANI/graphene has showed enhanced current density with quick response and a linear concentration range of 10 to 300 μM for UA and 30 to 80 μM for AA. These flexible sensor strips may be of great potential in real-time UA and AA detection.

Keywords: Polyaniline, Graphene, Uric acid, Ascorbic acid, Electrochemical biosensor

Over the past decade, there is a huge research interest towards the fabrication of simple and disposable biosensors with fast response time. A biosensor is an analytical device which can convert a biological response into a signal which is quantifiable and processable. The first try to produce such sensors was given by Clark and Lyons back in 1962 for glucose sensing^{1,2}. Based on the materials and techniques used, the biosensors are classified into several types, and one among them is electrochemical biosensor. In an electrochemical biosensor, the biological event like in the reaction type is directly converted to a measurable electronic signal, making them specific, sensitive and highly selective towards the detection of various biomolecules. The biosensor is made of two components, namely, a bioreceptor and a transducer. The receptor distinctly binds to analyte (like antigens, nucleic acids, binding protein, enzymes etc); an interface architecture wherein a particular biological event takes place, due to signal is generated; signal is picked up by transducer element (this can be an optical, electrochemical or a piezoelectrical device); transducer signal gets converted to an electronic signal and detector amplifies this signal, computer software then converts it to a meaningful physical parameter and

finally gets presented to human operator through interface. Bioreceptor and transducer together, sometimes are called as biosensor membrane^{3,4}. The simplicity of the electrochemical method makes it more attractive towards biomolecule detection. In humans and the higher primates, purine metabolism gives the prime end product, the uric acid (UA), which is excreted as the urine. In a healthy human, the average amount of UA present in the urine is 1.4 - 4.4 mM and that in blood is 120-450 μM ⁵. Hyperuricemia, gout and also cardiovascular diseases are caused due to the increased level of UA in the blood. Decreased level of them is seen in patients having Wilson's disease and Fanconi syndrome⁶. Thus, the monitoring of UA becomes very important. Ascorbic acid (AA) is a vital soluble vitamin that is generally used as a supplementary for the inadequate intake. The use of AA is extended towards a wide range of application like in treatment for common cold, infertility and mental illness. It also protects the cell from radical damage and hence acts as an antioxidant. The reduced intake causes scurvy. The high intake leads to digestive distress like diarrhoea and nausea. Since the AA related to disease states their quick detection has to be done for disease diagnosis.

Polyaniline (PANI), a promising conducting polymer, has good chemical stability in acidic solution, easy processability leads to low cost, and shows relatively good conductivity in the partially oxidized state⁷. Different techniques are used to provide electrode surfaces possessing sensing abilities for monitoring glucose. Development of immobilized glucose is based on conducting polymers which acts as a new class of the electrode materials providing a satisfactory platform for biological analyte detection. PANI, a conducting polymer is of scientific and technological interest. Biomolecules including proteins, DNA, enzymes have shown excellent performance on immobilization upon modified PANI electrode⁸. PANI synthesis is quite an easy method. Further, PANI and its derivatives exhibit variety of properties such as biocompatibility, stability, good electrical conductivity, bind with enzymes covalently and can be easily processed. Different forms of PANI possess different colours, and they differ in stability and conductivity. PANI is found in one of three oxidation states, namely, leucoemeraldine – colourless (C_6H_4NH)_a; emeraldine – green for salt; blue for the base ($[C_6H_4NH]_2[C_6H_4N]_2$)_n; (per)nigraniline – blue/violet (C_6H_4N)_n. Polyaniline only on protonation form emeraldine salt that can conduct electricity⁹. To enhance the properties of PANI it is made composite with other functional materials. 2-D sheet of graphene is one such material, with one-atom-thickness. It is composed of carbon, which is woven in a honeycomb structure. Graphene possesses a number of applications in various fields including batteries, transistors, touch screens, solar cells, even applied in the construction of strong materials like aeroplanes, satellites, cars and also for constructing biosensors^{10,11}. Graphene is applied on to a wide range of biosensors, in specific affinity-based biosensor like immunosensors, DNA sensors. Graphene is chosen as the biosensors as they possess large specific surface area, good elasticity and thermal conductivity, high mechanical strength, higher electron mobility even at room temperature, tuneable bandgap and even possess high electrical conductivity. Along with these they even have a low environmental impact. Graphene has the ability to be functionalized by both covalent bonding as well as non-covalent bonding of small molecules providing compatibility for biological receptors immobilization^{12,13}.

In the present work, we demonstrate the modification of flexible and non-conducting overhead polyester sheets into conducting films by the silar deposition¹⁴ technique. PANI was then coated on

them through oxidation of aniline. The coating is optimized through electrochemical impedance spectroscopy. On another side of the strip, graphene is coated with the help of the binder. The oxidation of aniline to PANI is confirmed through UV-visible spectroscopy. The formation of PANI and composite of PANI/graphene was confirmed using scanning electron microscopy. This strip of PANI/graphene is used for the detection of UA and AA in phosphate buffer (pH = 7.2) using cyclic voltammetry (CV) and chronoamperometry (CA) techniques.

Materials and Methods

Commercially available polyester overhead projector (OHP) sheets of thickness 50 μ m were purchased from the local providers. 3-aminopropyltrimethoxysilane (APTMS), UA and AA were purchased from Nice chemicals Pvt. Ltd, Sigma Aldrich, and Loba Chemicals, respectively. Graphene platelet nanopowder was procured from Sisco Research Laboratory Pvt Ltd.

Modification of OHP sheets

The OHP sheets are cut in the dimensions of 1 \times 8 cm, cleaned in acetone, ethanol and distilled water through ultrasonication for 15 min in each. The strips are then dried. The mixture of H₂SO₄ and H₂O₂ in the volume/volume ratio of 3:1 is termed as piranha solution. The cleaned strips are dipped in the piranha solution for about 5 min and dried. The strips are later dipped in ethanol for 20 min and when dried are placed in APTMS solution (95 mL ethanol : 5 mL water: 2 mL APTMS solution) for 20 h. These strips are then washed with ethanol and water and later kept for drying¹⁵.

Deposition of PANI and graphene on the modified OHP

The procedure for the deposition of PANI film on the APTMS modified OHP sheet was done by oxidative chemical polymerization technique. Two beakers, B₁ containing cationic precursor and B₂ containing anionic precursor were taken. The cationic precursor is a mixture of 50 mL of 0.1 M aniline in distilled in 50 mL of 1 M sulphuric acid and the anion precursor is the mixture of 50 mL 0.1 M ammonium persulfate. The APTMS modified dried strips are immersed in each solution for 30 s, this completes one cycle¹⁶. The dipping is continued and after every 100 cycles, electrochemical impedance spectroscopy (EIS) is taken to optimize the number of cycles with lesser resistance value for better conductivity. As the course of time, the formation of the greenish layer is

observed. This greenish layer is due to the formation of emeraldine form of PANI. 1000 cycles were completed to get the lesser resistance of the film. The strip is allowed for drying.

The graphene is ground well with the binder (poly(vinylidene fluoride) + N-methylpyrrolidone). The well grinded slurry is then coated on one side of the PANI deposited strip and dried. A drop of silver paste is applied on both the sides of the strip and at the junction of the PANI and PANI/graphene composite for connecting to a potentiostat. This strip will act as working electrode, for sensing of UA and AA. The entire process is represented in the schematic representation as shown in Fig. 1.

Material characterization

The oxidation chemical polymerization of PANI was confirmed through Fourier transform infrared spectroscopy (FTIR, Shimadzu) and ultraviolet-visible spectroscopy (UV-VIS, Double Beam Spectrophotometer 2201). The surface morphology of the deposited PANI and PANI/graphene was analyzed with scanning electron microscope (SEM, ZEISS EVO18 special edition).

Electrochemical characterization

To optimize the deposition of PANI on the modified OHP strips, Nyquist plots from EIS was

obtained. For the detection of UA and AA in the phosphate buffer (pH = 7.2), standard electrochemical techniques like cyclic voltammetry (CV) and chronoamperometry (CA) measurements were carried out in a three-electrode setup, using the electrochemical workstation BioLogic SP-150. Pt as the counter, saturated calomel electrode as the reference and PANI/graphene modified OHP strips as the working electrode was chosen for all the measurements. CA experiments were performed by measuring the current with respect to time at a fixed potential for each addition of UA or AA.

Results and Discussion

The morphology of (a) graphene, (b) PANI and (c) PANI/graphene modified OHP sheets were analyzed through SEM (Fig. 2). The procured graphene was made up of few layers of graphene termed as graphene flakes (Fig. 1a). PANI exhibits interconnected granular morphology as shown in Fig. 1b. This granule formation of PANI can be accounted for the heterogeneous nucleation of aniline and the reaction temperature. During the initial cycles, the colour of the strip was observed to be bluish in nature. But as the number of cycles increased for deposition the bluish colour of the strip slowly changes to emerald green. The reason behind this is the formation of emeraldine base, which is blue in colour.

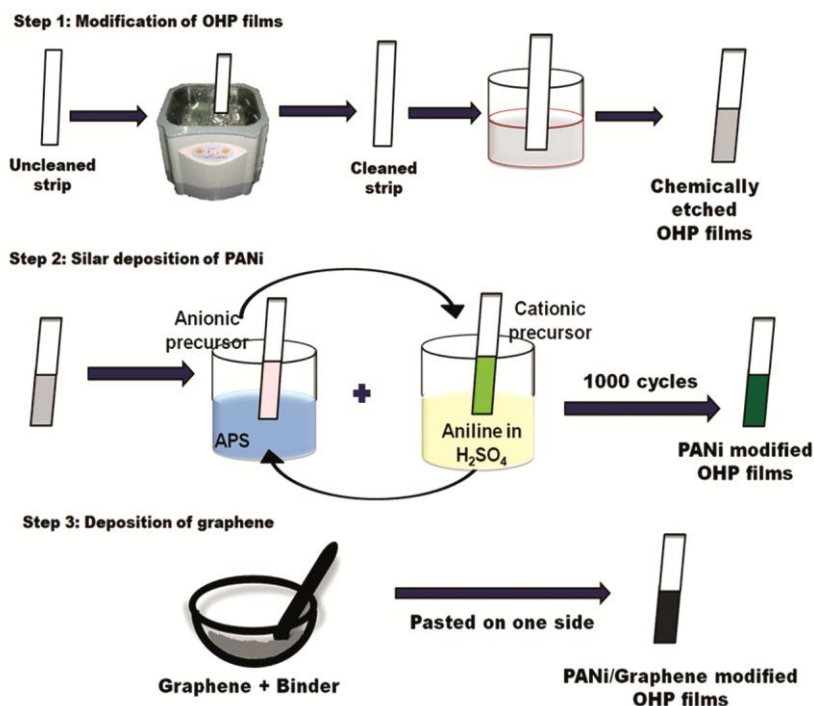


Fig. 1 — Schematic representation of a modification of OHP strips into PANI/graphene modified OHP strips

When the deposition is been carried out initially, the colour was found to be blue. As the deposition time and layers increases, the oxidation of polyaniline (PANI) increases which in turn changes the colour to green. The emeraldine salt of PANI is formed during protonation of the emeraldine base with organic and inorganic acids (H_2SO_4 in the present case). This process is referred to as doping. When PANI in the form of the emeraldine base is treated with acids, protons primarily interact with the imine atoms of nitrogen; as a result, polycations appear. Because positive charges are localized on neighbouring nitrogen atoms, there is increase in the total energy of the polymer system, electron density tends to undergo redistribution; as a consequence, “unpairing” of the lone pair of electron of the nitrogen atoms occurs without any change in the amount of electrons in the system. During the initial stage of polymerization of aniline on the substrate surface, there are no other nuclei available for the heterogeneous polymerization. Thus, the PANI on the

strip is bluish in colour. But as the number of cycles is increased, the newly polymerized aniline-PANI has now an old PANI nucleus for its growth. i.e., the heterogeneous polymerization process is said to occur¹⁷⁻²⁰. The entire process of doping and undoping mechanism of PANI in acidic and basic media is shown in Scheme 1. This heterogeneous nucleation further causes the agglomeration of the initially formed fibres giving rise to the densely formed granular morphology at the end of 1000 cycles as evident from Fig. 2b and thus, the green colour of PANI on the modified OHP sheets. While in PANI/graphene, the graphene flakes and the granule morphology of PANI coexists (Fig. 2c). This shows the clear deposition of graphene nanoflakes on the predeposited PANI.

The FTIR spectra of PANI are shown in Fig. 3a. The nonconducting OHP sheets are modified into conducting strips using APTMS. This coating of APTMS on the OHP strip is confirmed through the peaks at 1288 and 1068 cm^{-1} . The stretching

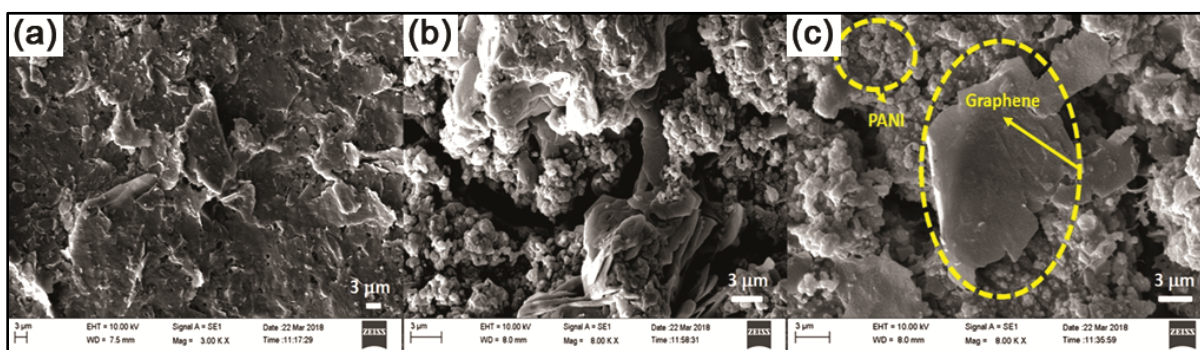
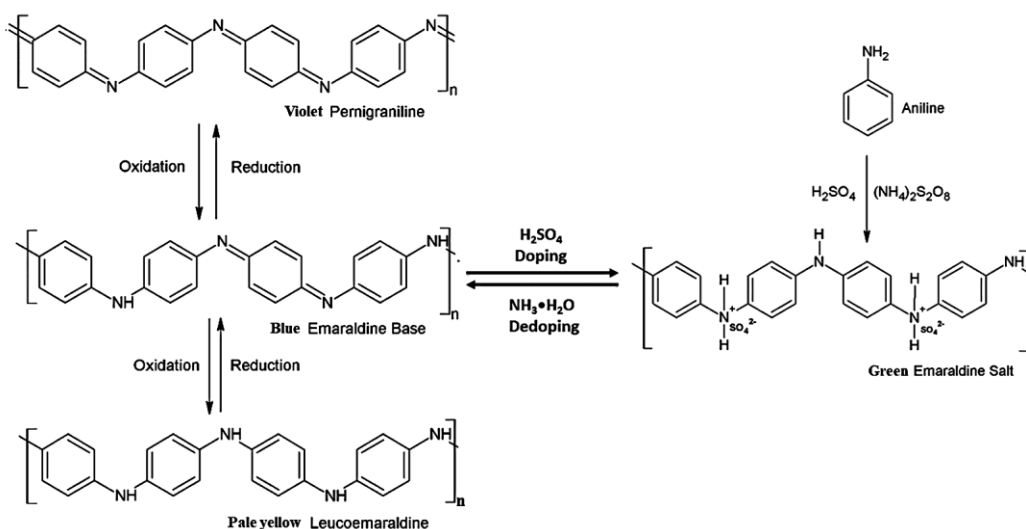


Fig. 2 — SEM images (a) graphene, (b) PANI and (c) PANI/ graphene modified OHP strip.



Scheme 1 — The doping and dedoping mechanism of PANI in acidic/basic medium.

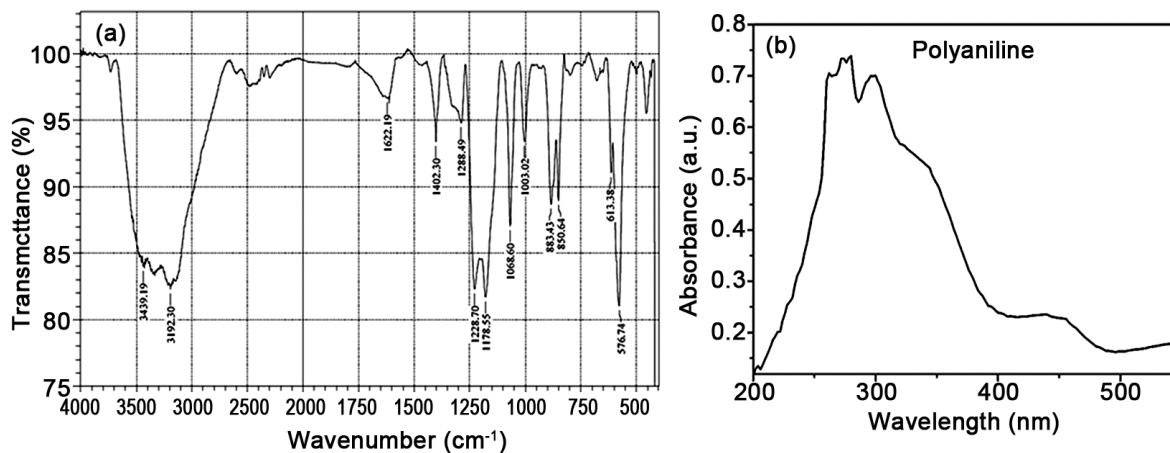


Fig. 3 — (a) FTIR spectra of PANI and (b) UV-Vis absorption spectra of PANI.

vibrations of Si-CH₂ and Si-O-Si functional groups of the APTMS are indexed to the bands at 1288 and 1068 cm⁻¹, respectively. PANI exists in three different forms of oxidation states: leuco emeraldine, emeraldine, and pernigraniline²¹.

To understand the structure of PANI, it is important to know the most important parts of it, i.e. the conjugated double bond structure, the benzenoid amine, and the quinoid imine. The characteristic bands for PANI observed in the spectrum 2a are 3439, 1622, 1402, 1288, 1228, 1178, 1068, 1003, 883, 850, 613 and 576 cm⁻¹. The broad band at 3439 cm⁻¹ is indexed to the stretching modes of N-H of the amino group. The peaks at 1622 and 1402 cm⁻¹ are due to the presence of the C=C of the quinonoid ring and the C=C of the benzenoid rings, respectively. The band at 1288 cm⁻¹ in the spectrum corresponds to the C-N stretching vibrations of the secondary aromatic amine, which is a measure of the degree of electron delocalization as an “electronic-like bond”. This C=N bond is of prime interest to confirm that if the PANI is in the doped state. 850 cm⁻¹ band is observed due to the C-H out of plane bending vibration and 883 cm⁻¹ band due to the C-H in-plane bending vibrations. The band around 3500 cm⁻¹ shows the peak of N-H stretching. The peak at 1178 cm⁻¹ that is indexed to the B-NH⁺=Q vibration, indicates the conductive behaviour of PANI. Further, it also signifies the positive charge exists on the chain and also the distribution of the dihedral angle between the quinonoid and benzenoid rings. With the increase in the degree of protonation of the PANI backbone, the absorption band also increases. This is evident to the high degree of electron delocalization in PANI,

accompanied by the strong interchain NH⁺-N hydrogen bonding. The successful polymerization of aniline into the green protonated emeraldine form of PANI is confirmed through all the mentioned absorption bands that are distinctive of PANI²².

The UV-visible spectrum of the synthesized PANI (Fig. 3b) is recorded by dispersing PANI in dimethylsulphoxide solvent. It shows two characteristic peaks at around 300 and 400 nm. The 300 nm peak corresponds to benzenoid rings π-π* transition. The peak at 450 nm is assigned to the localized polarons transitions which are characteristics of the protonated PANI. A weak peak at 370 nm is attributed to the n-π* transitions of the benzenoid ring.

Electrochemical characterization

The EIS measurements for the prepared working electrode are represented with the Nyquist plot (Fig. 4) The Nyquist plot for the deposition of PANI on the modified OHP sheets. The nyquist plot in the present study has two significant sections, namely, the intercept of the impedance curve on the real axis at high frequency region and a linear curve in a low frequency region. EIS is observed due to the bulk resistance of the electrolyte, the inherent resistance of the electrode active material along with the contact resistance at the interface between electrolyte and electrode. However, the arc in the low-frequency region of the Nyquist plot clearly indicates the charge transfer resistance of the electrode material resulting from the diffusion of electrons. The reduced width of the semicircle loop in the low-frequency region is due to the shortened path for electron transport within the

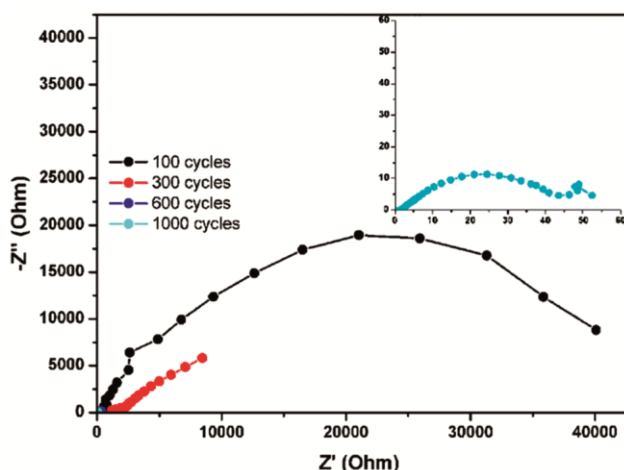


Fig. 4 — Nyquist Plot obtained from electrochemical impedance spectroscopy for the deposition of PANI on the APTMS modified OHP sheet at different cycles.

electrode material. As the number of cycles for the deposition of PANI increases, the resistance value slowly decreases. This is evident from Fig. 4a. Initially, when 100 cycles were completed for deposition, the resistance value was found to be 15000 Ω . But with the increases in the deposition cycles the resistance value slowly started decreasing and finally, by the end of the 1000 cycles, the resistance was 150 Ω . With further increase in the number of cycles, it was noticed that the deposited PANI on the modified OHP strips started peeling out and hence, 1000 cycles deposition was taken to be optimal. The graphene then was coated on both the sides of the PANI strips using a binder. This strip gave a higher impedance value than the strip where graphene was coated on the single side. Thus further, the deposition of the graphene on the single side was taken to be an optimum. Therefore, the strip having one side PANI and the other side PANI/graphene is taken to be the working electrode for the current study. From the inset plot (Fig. 4) we could observe the Nyquist plot containing a semicircle loop at the higher frequency region. This in simple terms represents the internal resistance between the electrode material and the electrolyte. The reduced path of the arc indicates the shortened way for the e^- transport within the electrode-electrolyte interface. The conductivity of PANI depends upon the level of doping and the doping is further dependent on the polymer's oxidation. The extended delocalized bonds of PANI mainly composed of aromatic units which in turn acts similar to that of the silicon bond structure with the localized state. Conducting polymers are

regarded to have low conductivities but the doping process induces the charge carriers. These move under the effect of the applied electric field which further is responsible for the enhanced conductivity of PANI. On making a composite with the few-layer graphene, the conductivity of PANI is greatly influenced, with the reduced resistance of the composite as shown in the Fig. 4. This enhancement in the conductivity of the polymer can be held responsible for the additional conductivity of graphene.

Fig. 5 represents the CV response of PANI/graphene electrode with and without the presence of uric acid in the 0.1 M phosphate buffer (pH = 7.2) and Fig. 6 represents that of ascorbic acid response at a scan rate of 50 mVs^{-1} . As we can notice the PANI/graphene electrode showed an enhancement in the current density in the presence of both UA and AA. But compared to the AA, the uric acid response was much higher. The PANI/graphene redox sites that are available show a significant catalytic behaviour. The effect of the different scan rates towards the electrocatalysis behaviour of UA and AA at the PANI/graphene electrode was studied as represented in Fig. 5b and 6b, respectively. The current density of both UA and AA increased linearly with the increase in the scan rates. There was no any altered behaviour with the different scan rates applied. This shows a good linearity which further indicates that the catalytic behaviour is due to the surface-confined diffusion process.

Determination of UA and AA by voltammetry and amperometry

Fig. 5c and 6c represent the CV response obtained at the PANI/graphene electrode in the 0.1 M phosphate buffer containing different concentrations of UA and AA, respectively. There is no CV response for both UA and AA at a lower concentration of about 10 μM of the same, respectively. But as the concentration of UA and AA is increased the CV response starts changing. In the case of UA detection, the response starts changing when the concentration of the UA is increased to 20 μM . While in the AA detection, the CV response changes when the concentration of AA is increased to 30 μM in the phosphate buffer electrolyte. As the concentration of uric acid was varied from 2 μM to 1 mM there was a slow increase in the current. From the CVs of UA at the modified electrode there is no reduction peak of UA, only its oxidation peak is observed, which

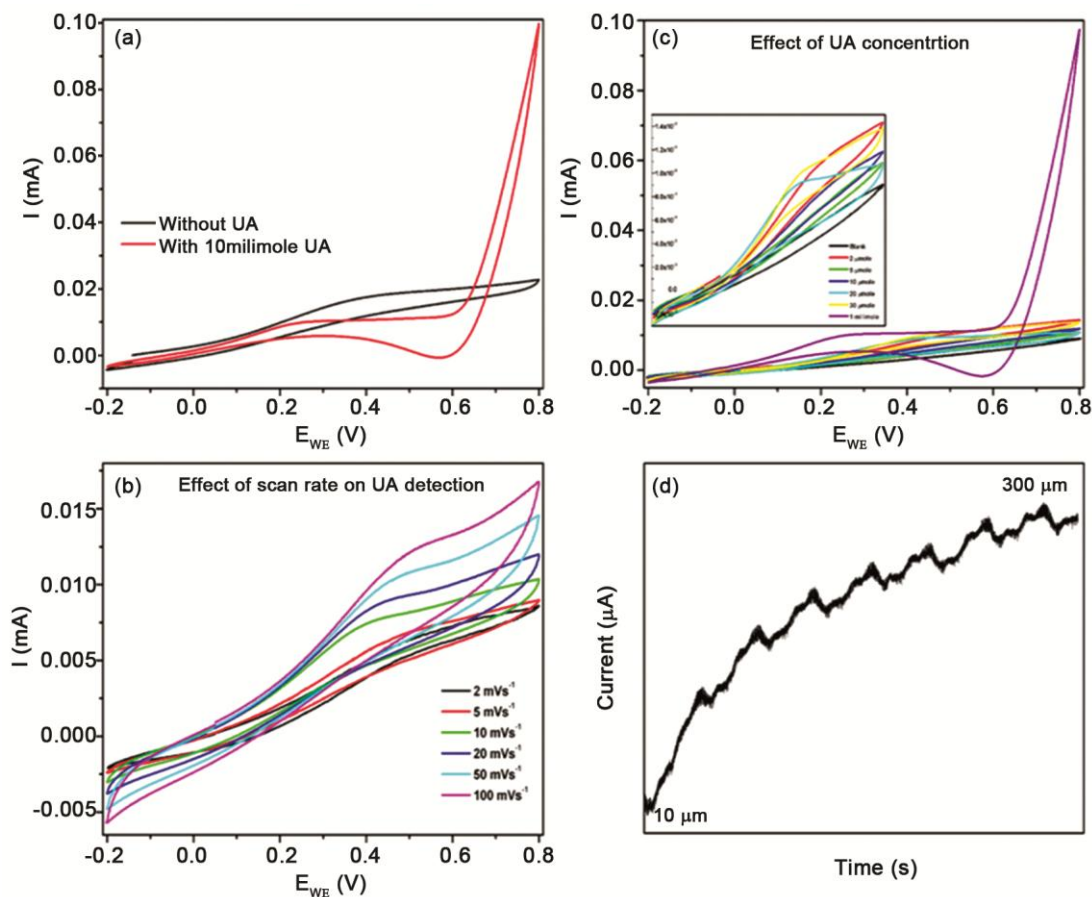


Fig. 5 — CV for PANI/Graphene modified OHP strip in phosphate buffer of pH=7.2 (a) with and without the presence of UA, (b) containing different concentrations of UA, (c) effect of scan rates towards 20 μM UA at different scan rates ranging from, 2 to 100 mVs^{-1} and (d) amperometric response obtained at fixed potential during incremental addition of UA.

demonstrates that the reaction is irreversible. In AA detection the lowest volume of 20 μM was detected but as a concentration of it was increased there was no significant difference in the peak height except a little increase in the peak height however at a higher concentration a clear-cut AA detection is seen through the increase in the peak at 10 mM concentration. In order to further study the sensitivity of UA and AA determination, amperometry method was adapted. The amperometric curve for the PANI/graphene electrode for sequential addition of UA acid in the phosphate buffer (Fig. 5d) is recorded in the time interval of 100 s and Fig. 6d represents the sequential addition of AA. The applied potential for UA detection was +0.32 V and for that of AA was +0.18 V and very slow rotation of 200 rpm was maintained throughout the amperometric studies so as to not disturb the electrode setup. The current density for each incremental addition of UA and AA increased with the course of time. As we can see in

the Fig. 5c and 6c, with the addition of UA and AA there is a sudden increase in the current density and then attains the stability. Corresponding variations in the current density values were plotted and shown in Fig. 5d and 6d. The linear detection range for the PANI/graphene in case of UA was found to be 10 μM to 300 μM and for that of AA was found to be 30 μM to 80 μM . Table 1 summarises the sensing performance of the present work with the literature. Due to the continuous reaction between PANI/graphene strip during UA/AA sensing, the PANI loses its emerald green colour and turns to brown at the end of the reaction. The PANI is completely oxidized by the end of the reaction. This shows effective sensing ability of PANI/graphene strips towards the biomolecule (UA/AA) sensing. Thus, these PANI/graphene modified OHP strips can be used as one-time use strips for real-time applications. After the detection of UA/AA these strips can be discarded.

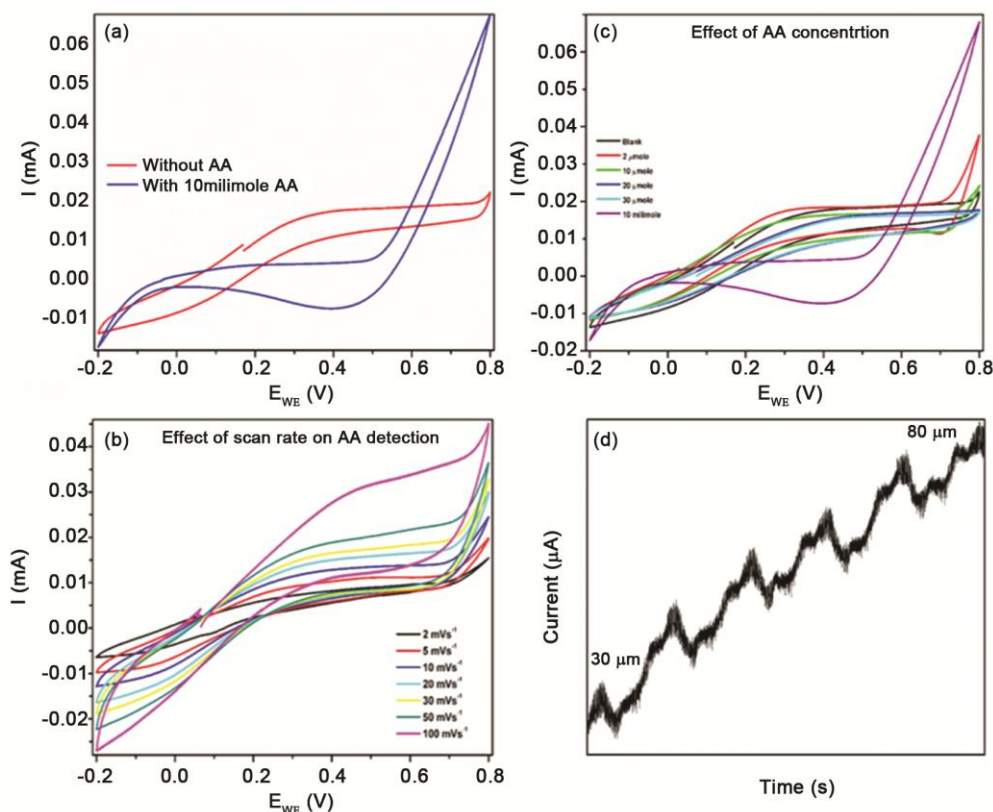


Fig. 6 — CV for PANI/graphene modified OHP strip in phosphate buffer of pH=7.2 (a) with and without the presence of AA, (b) containing different concentrations of AA, (c) effect of scan rates towards 30 μM UA at different scan rates ranging from, 2 to 100 mVs^{-1} and (d) amperometric response obtained at fixed potential during incremental addition of AA.

Table — 1 Comparison of the present work with the reported work on other electrochemical methods for the detection of UA and AA at PANI/Graphene modified OHP sensor strip

Electrode	Molecules Detected	Range of detection	Detection Limit	Ref.
PANI-Fe	UA	0.05 – 3860 μM	21.5 μM	[5]
Tryptophan/Graphene	UA	10 – 1000 μM	5.3 μM	[23]
Tapered plastic optical fiber coated with graphene polymer composite	UA	--	7.61 ppm	[24]
PANI/Prussian-Blue	UA	10 – 160 μM	160 μM	[25]
PANI/Poly(allylamine)	UA	--	--	[26]
Graphene/GC	AA	10 – 6000 μM	3.00 μM	
	UA	0.60 – 120 μM	0.080 μM	[27]
Graphene modified electrode	UA	0.012 – 2.00 μM	60 μM	[28]
MoS ₂ /PEDOT	AA	20 – 140 μM	5.83	
	UA	2 – 25 μM	0.95	[29]
Graphene Oxide-templated PANI micro sheets	AA	150-1050 μM	--	
	UA	3-26 μM	--	[30]
PANI-Halloysite nanotubes	AA	0.005 – 5.5 mM	0.21 μM	[31]
PEDOT-Au	AA	500 – 3500 μM	--	[32]
	UA	20 – 130 μM	--	
TiO ₂ - PEDOT	AA	6 – 46 μM	20 nM	[33]
RGO-Ag/PANi/GCE	UA	20-350 μA	0.2 μA	
	AA	50 -1000 μA	0.5 μA	[34]
Graphene ink	UA	0.5 – 150 μM	0.29 μM	
	AA	50 – 1000 μM	17.8 μM	[35]
PANI/graphene modified OHP strips	AA	10 – 300 μM	--	Present Work
	UA	30 – 80 μM	--	

Conclusions

In this work a flexible, a disposable and low-cost sensor strips for uric acid and ascorbic acid detection are prepared and demonstrated. PANI modified OHP sheets were prepared through SILAR deposition technique. Graphene with the help of binder is deposited on one side of the PANI modified OHP sheet. The deposition of the PANI on the modified OHP sheets were monitored through EIS and the morphology was analyzed through SEM. The electrochemical studies revealed that the composite has electrocatalytic ability towards oxidation of uric acid and ascorbic acid. The PANI/graphene-modified electrode exhibited excellent electrocatalytic activity towards uric acid and ascorbic acid electrochemical oxidation, which may be attributed to the active PANI/graphene surface. The biosensor exhibited major advantages for the detection of uric acid at a low potential. Detection limit range of 10–300 mM for uric acid and 30–80 μ M for ascorbic acid was achieved on PANI/graphene. Thus, in the current study, we report the disposable UA/AA sensor strips which will be well suited for the real-time applications.

Acknowledgement

The author owes her gratitude to Manipal Institute of Technology for the laboratory and the instrumental facility rendered.

References

- Koyun A, Ahlatcioglu E & Ipek Y K, *Biosensors and their Principles*; Ed. by S. Kara, Intech Open, London (2012) 115.
- Pohanka M & Skladal P, *J Appl Biomed*, 6 (2008) 57.
- Xiang Q, *ICCC*, 235 (2011) 215.
- Hammond J L, Formisano N, Estrela P, Carrara S & Tkac J, *Essays Biochem*, 60 (2016) 69.
- Govindasamy M, Mani V, Chen S-M, Sathiyar A, Merlin J P & Ponnusamy V K, *Int J Electrochem Sci*, 11 (2016) 8730.
- Wyngaarden B J & Kelly N W, *Guot and Hyperuricemia*, Grune and Stratton, New York (1974) 1000.
- Li D, Huang J & Kaner R B, *Acc Chem Res*, 42 (2009) 135.
- Tahira Z M, Alociljaa E C & Grooms D L, *Biosens Bioelectron*, 20 (2005) 1690.
- Boeva Z A & Sergeev V G, *Polym Sci Ser C*, 56 (2014) 144.
- Loh K P, Bao Q, Ang P K & Yang J, *J Mater Chem*, 20 (2010) 2277.
- Huang X, Qi X, Boeyab F & Zhang H, *Chem Soc Rev*, 41 (2012) 666.
- Georgakilas V, Tiwari J N, Kemp K C, Perman J A, Bourlinos A B, Kim K S & Zboril R, *Chem Rev*, 116 (2016) 5464.
- Ambrosi A, Chua C K, Bonanni A & Pumera M, *Chem Rev*, 114 (2014) 7150.
- Deshmukh P R, Patil S V, Bulakhe R N, Sartale S D & Lokhande C D, *Mater Today Commun*, 8 (2016) 205.
- Thota R & Ganesh V, *Analyst*, 139 (2014) 4661.
- Patil S S, Koiry S P, Veerender P, Aswal D K, Gupta S K, Joaga D S & More M A, *RSC Adv*, 2 (2012) 5822.
- Wang Y & Jing X, *J Phys Chem B*, 112 (2008) 1157.
- Huang J, Virji S, Weiller B H & Kaner R B, *J Am Chem Soc*, 125 (2003) 314.
- Tran H D, Wang Y, D'Arcy J M & Kaner R B, *ACS Nano*, 2 (2008) 1841.
- Huang J & Kaner R B, *Angew Chem*, 116 (2004) 5941.
- Huang J & Kaner R B, *Chem Commun*, 36 (2006) 367.
- Mu S & J. Kan, *Synth Met*, 98 (1998) 149.
- Sun C-L, Lee H-H, Yang J-M & Wu C-C, *Biosens Bioelectron*, 26 (2011) 3450.
- Batumalay M, Harun S W, Ahmad F, Nor R M, Zulkepely N R & Ahmad H, *IEEE Sens J*, 14 (2014) 1704.
- Thakur B & Sawant S N, *ChemPlusChem*, 78 (2013) 166.
- Wathoni N, Hasanah A N, Gozali D, Wahyuni Y & Fauziah L L, *J Adv Pharm Technol Res*, 5 (2014) 13.
- Chen M F & Ma X Y, *Russ J Appl Chem*, 87 (2014) 200.
- Chao M, Ma X & Li X, *Int J Electrochem Sci*, 7 (2012) 2201.
- Li Y, Lin H, Peng H, Qi R & Luo C, *Microchim Acta*, 183 (2016) 2517.
- Bao Y, Song J, Mao Y, Han D, Yang F, Niu L & Ivaska A, *Electroanalysis*, 23 (2011) 879.
- Shao L, Wang X, Wang Q, Tian Q, Ji Z & Zhang J, *Electrochim Acta*, 255 (2017) 286.
- Phongphut A, Sriprachuabwong C, Wisitsoraat A, Tuantranont A, Prichanont S & Sritongkham P, *Sens Actuator B*, 178 (2013) 501.
- Soundappan T, Rajkumar M & Chen S-M, *Int J Electrochem Sci*, 7 (2012) 2109.
- Guo Z, Luo X, Li Y, Li D, Zhao Q, Li M, Ma C & Y. Zhao, *Chem Res Chi Uni*, 33 (2017) 507.
- Fu L, Wang A, Lai G, Su W, Malherbe F, Yu J, Lin C-T & A. Yu, *Talanta*, 1 (2018) 248.